

# Effect of CLC-2 on the cytoskeleton in human trabecular meshwork cells

HONG WEI WANG<sup>1,2</sup> and YA JUAN ZHENG<sup>1</sup>

<sup>1</sup>Department of Ophthalmology, The Second Hospital of Jilin University, Jilin University, Changchun, Jilin 130041;

<sup>2</sup>Department of Ophthalmology, The First Affiliated Hospital of Qiqihar Medical College, Qiqihar Medical University, Qiqihar, Heilongjiang 161041, P.R. China

Received November 22, 2012; Accepted August 1, 2013

DOI: 10.3892/mmr.2013.1619

**Abstract.** The chloride channel protein 2 (CLC-2) is important in maintaining the volume of trabecular meshwork cells by adjusting the outflow of aqueous solutions and maintaining the fluid balance. However, little is known concerning the functions of CLC-2 in the cytoskeleton, specifically in human trabecular meshwork (HTM) cells. In the present study, two CLC-2 specific siRNAs (siRNA1 and siRNA2) that target CLC-2 mRNA were designed. The siRNAs were transfected into the HTM cells and the results showed that siRNA1 in particular decreased the expression of CLC-2 by ~45%. Furthermore, an siRNA1-mediated CLC-2 knockdown significantly reconstructed the actin cytoskeleton and formed cross-linked actin networks. In addition, the downregulation of the expression of CLC-2 was associated with increased TGF- $\beta$  and Smad2 activities in the HTM cells following 24 h of transfection. In conclusion, these results suggest that CLC-2 knockdown promotes trabecular meshwork cytoskeletal disorders and may activate the TGF- $\beta$ /Smad signaling pathway. Thus, CLC-2 may be a promising and potential novel therapeutic strategy for combating primary open-angle glaucoma.

## Introduction

Glaucoma is the most common cause of irreversible blindness worldwide. It is an optic neuropathy characterized by structural damage to the optic nerve and the associated visual dysfunction that may be caused by various pathological processes (1). The most common form of glaucoma is primary open-angle glaucoma (POAG), in which a high intraocular pressure is the most critical risk factor in the pathogenesis. The early onset of POAG is asymptomatic and the majority of patients

only seek medical treatment when visual function has been damaged (2). The treatment of POAG involves reducing the intraocular pressure to protect the residual vision. Therefore, the elucidation of the pathogenesis of primary open-angle glaucoma and the development of effective treatments have become top priorities.

Rapid developments in cell and molecular biology in recent years have revealed that the intraocular pressure in POAG is caused by a resistance to the aqueous outflow, which comes primarily from the trabecular meshwork (TM) (3). The form, number of changes, decline in the phagocytic function, extracellular matrix deposits, abnormal cell connections, actin cytoskeleton and cell shrinkage status of the TM cells also affect the actin cytoskeleton (4). Increasing the crosslinking of the actin cytoskeleton may reinforce the TM and increase the aqueous outflow; however, this increased outflow may result in an obstruction and increase the intraocular pressure, thereby damaging the normal structure and function, and leading to the development of POAG (5,6). Therefore, an investigation of the characteristics of the TM cells in culture is important in the study of the pathogenesis of glaucoma.

In recent years, the number of studies concerning the ion channels formed in POAG, particularly the involvement of chloride channels has increased. Chloride channels (CLCs) are widely distributed in mammalian organs and cells, and function to maintain the volume of cells, adjust the cell electrical activity balance and mediate cell migration and other functions that impact cell physiology and pathology (7,8). Several chloride channels have been cloned, including CLC-1 to CLC-7, CLC-ka and CLC-kb. TM cells express CLC-2, CLC-3 and CLC-5. However, in TM cells, CLC-2 is the most prevalent channel of the CLC family and is upregulated following cell swelling (9). This channel is activated by membrane hyperpolarization in other cell types; due to the activation of CLC-2 by cell swelling, this protein has been implicated in cell volume regulation (10-12). In addition to cell swelling, CLC-2 may be involved in several cell mechanisms, including signal transduction, transepithelial transport, phagocytosis and membrane potential stabilization. In addition, CLC-2 may be important in maintaining the volume of TM cells by adjusting the outflow of aqueous solutions and maintaining the fluid balance (13). However, little is understood concerning the functions of CLC-2 in the cytoskeleton in TM cells.

---

*Correspondence to:* Dr Ya Juan Zheng, Department of Ophthalmology, The Second Hospital of Jilin University, Jilin University, 218 Ziqiang Street, Changchun, Jilin 130041, P.R. China  
E-mail: zhengyajuan124@yahoo.com.cn

**Key words:** siRNA, chloride channel protein 2, cytoskeleton, human trabecular meshwork cells

In the present study, human TM cells (HTM) were cultured to investigate the effects of CLC-2 on the function and restructuring of the cytoskeleton to clarify the effects of CLC-2 on the pathogenesis of POAG.

## Materials and methods

**siRNA design.** The candidate nucleotide sequence for the siRNA was obtained by searching the nucleotide sequences of CLC-2 using the Rational siRNA Design program (Qiagen, Hilden, German). A scrambled siRNA with the same nucleotide composition as the siRNA, but lacking significant sequence homology to the genome, was also designed. These oligonucleotides were ligated into the siXpress Human U6 PCR vector system (Mirus Bio, Madison, WI, USA) according to the manufacturer's instructions. The sequences of the siRNAs targeting CLC-2 were as follows: Sense: 5'-TCCTGTGAGAAGCTTCTCAC-3' and anti-sense: 5'-GTGAGAAGCTTCTCACAGGA-3' for siRNA1; sense: 5'-CCATGCTTATGTCACCAG-3' and antisense: 5'-GGTACGAAATCACAGAGTGGTC-3' for siRNA2; and sense: 5'-CACTCTTCGAAGAGTGTCT-3' and antisense: 5'-GTGAGAAGCTTCTCACAGGA-3' for scRNA.

**Cell line and cell culture.** HTM cells highly express CLC-2. The cell line was purchased from ScienCell (ScienCell Research Laboratories, San Diego, CA, USA). The cells were maintained and cultured in Dulbecco's modified Eagle's medium (DMEM) supplemented with 10% fetal bovine serum (ScienCell Research Laboratories), 100 IU/ml penicillin, 100 IU/ml streptomycin and 2 mmol/l L-glutamine in a humidified 5% CO<sub>2</sub> atmosphere at 37°C (14). The cells were counted in suspensions using a Cedex analyzer (Innovatis AG, Bielefeld, Germany).

**Transfection.** The transfection was performed in a Lipofectamine 2000 system (Invitrogen Life Technologies, Grand Island, NY, USA), according to the manufacturer's instructions, using a 5 µl expression vector in 250 µl serum-free medium. The concentration of each siRNA used was 100 pmol in 250 µl medium (33 nM). After 6 h, the medium was replaced with fresh serum-containing DMEM and incubated for an additional 24 h.

**Real time-PCR.** Human CLC-2, actin, vinculin,  $\beta$ -catenin and  $\beta$ -actin (housekeeping gene, control) PCR primers were designed using Primer Express software (Perkin-Elmer Biosystems, Waltham, MA, USA) based on their published sequences (Table I). The total RNA of the HTM cells was isolated with TRIzol reagent (Invitrogen Life Technologies, Grand Island, NY, USA) according to the manufacturer's instructions. To avoid DNA contamination, the total RNA was treated with RNase-free DNase I (Takara, Kyoto, Japan) for 1 h at 37°C and extracted again with TRIzol reagent. The RNA purity was determined from the ratio of the absorbances at 260:280 nm and the RNA integrity was assessed by determining the intensity of the 28S and 18S rRNA bands following formaldehyde agarose gel electrophoresis. A sample of the total RNA (2 µg) was subjected to reverse transcription using the RevertAid™ First-Strand cDNA Synthesis kit (Fermentas

Inc., Glen Burnie, MD, USA) with a random hexamer primer and 2 µl cDNA solution was used for real-time PCR. The genes were amplified in a 25 µl reaction volume using SYBR-Green (Applied Biosystems, Foster City, CA, USA) on a MiniOpticon™ Real-time PCR System (Bio-Rad, Hercules, CA, USA). The temperature profile involved an initial denaturation step at 95°C for 5 min, followed by 40 cycles at 95°C for 10 sec, 58°C for 15 sec and 72°C for 10 sec, and a melting curve analysis was performed. The specificity of the amplified products was evaluated via agarose gel electrophoresis and was further verified with automated cycle sequencing. To ensure consistency in the threshold cycle (Ct) values, duplicate reactions were performed, and the mean Ct values were used for calculating the relative expression levels (14). The Ct values were analyzed as described previously by Zhou *et al* (15), and the normalized Ct values for each gene were subjected to Student's t-test with a two-tailed distribution to determine the statistical significance (95% confidence interval). The reactions were conducted in triplicate and the mean value was used. For standardization,  $\beta$ -actin was used as an internal control for each sample.

**Western blot analysis.** Following transfection, the cells were washed twice with pre-cooled phosphate-buffered saline (PBS) and 106 cells were treated with RIPA buffer [50 mM Tris (pH 8.0), 150 mM NaCl, 0.1% SDS, 1% NP40 and 0.5% sodium deoxycholate] containing a protease inhibitor (1% cocktail and 1 mM PMSF). The total proteins were separated on a 15% sodium dodecyl sulfate-polyacrylamide gel electrophoresis gel and transferred onto polyvinylidene fluoride (PVDF) membranes. The membrane was blocked with Tris-buffered saline containing 0.1% Tween 20 (TBST, pH 7.6) for 1 h at room temperature and the PVDF membrane was immunoblotted overnight at 4°C with a primary antibody solution (1:1000). Following two washes with TBST, the membrane was incubated with horseradish peroxidase-labeled secondary goat anti-mouse IgG2a-B antibody (sc-2073) for 1 h at room temperature and washed three times with TBST. The final detection was performed with enhanced chemiluminescence (ECL) western blotting reagents (GE Healthcare, Piscataway, NJ, USA) and the membranes were exposed to Lumi-Film Chemiluminescent Detection Film (Roche Applied Science, Rotkreuz, Switzerland) (16). The loading differences were normalized using a monoclonal  $\beta$ -actin antibody. The primary antibodies used in this study included anti-CLC-2 (SC-81871), anti-actin (SC-81760), anti-vinculin (SC-55465), anti- $\beta$ -catenin (SC-7963),  $\beta$ -actin (SC-130301), TGF- $\beta$  (SC-166833) and Smad2 (SC-101153). All antibodies were acquired from Santa Cruz Biotechnology, Inc. (Santa Cruz, CA, USA).

**Fluorescence microscopy.** The cells were fixed and subjected to immunofluorescent staining of the cytoskeletal proteins. Following a brief rinse in PBS at 37°C, the cells were fixed with 3% paraformaldehyde in PBS for 20-30 min at room temperature. Subsequent to fixation, the cells were rinsed with PBS and permeabilized with 0.5% Triton X-100 in PBS for 5 min. When a higher degree of permeabilization was required (e.g., for myosin II visualization in the HTM), the cells were initially fixed with a mixture containing 0.5% Triton X-100 and 3% paraformaldehyde in PBS for 2-3 min

Table I. PCR primers.

Gene	Primer sequences (from 5' to 3')	Product size (bp)
CLC-2	Forward: TCCTCACCCCTGGTCATCTTC Reverse: GCAGGTAGGGCAGTTTCTTG	402
Actin	Forward: GGTGAAGGTCGGAGTCAAC Reverse: CCATGGGTGGAATCATATTG	153
Vinculin	Forward: AAGCTGTCAAGCCGTGTTT Reverse: GCCTTCCGAGTCAGTTTCA	401
$\beta$ -catenin	Forward: AGGACTGGGTGCTGGTTATG Reverse: CAGCAGCTAGTCTCGCATTG	398
$\beta$ -actin	Forward: ATCATGTTTGAGACCTTCAACA Reverse: CATCTCTTGCTCGAAGTCCA	318

CLC-2, chloride channel protein 2.

and then post-fixed with 3% paraformaldehyde for 20 min. To visualize  $\beta$ -actin, the cells were subsequently incubated with 100 nM TRITC-phalloidin (Sigma-Aldrich, St. Louis, MO, USA). For antibody staining, the cells were incubated with primary antibodies diluted in PBS. The cells were then washed in PBS three times and incubated with the secondary fluorochrome-conjugated antibodies. The nuclei were stained with 2.5 mg/ml DAPI (Sigma-Aldrich), which was added to the secondary antibody solution (17). Following three final washes, the coverslips were mounted in Elvanol (Mowiol® 4-88; Sigma-Aldrich, Hoechst, Germany). The primary antibodies used for this method were the same as those used for the western blot analysis.

**Statistical analysis.** All the measurements were performed in triplicate and the results are expressed as the mean  $\pm$  SD. The data were obtained from at least three independent experiments. An analysis of variance for multiple comparisons was conducted using statistical analysis software (SPSS, Inc., Chicago, IL, USA).  $P < 0.05$  was considered to indicate a statistically significant difference (16).

## Results

**Inhibition of CLC-2 mRNA and protein expression by siRNA.** It was hypothesized that by preventing the transcription of CLC-2 mRNA via siRNA, the CLC-2 protein levels are significantly reduced. Real time-PCR and western blot analysis were used to detect the effects of CLC-2 on target gene expression in response to various concentrations (Fig. 1) to determine the optimal incubation concentration and the effect of the treatment length (Fig. 2).

Fig. 1A and B show that siRNA1 and 2 were able to inhibit CLC-2 mRNA and protein expression concomitantly. These effects were concentration dependent as the CLC-2 mRNA and the protein expression levels decreased with increasing concentrations of the siRNAs following 24 h of treatment. Furthermore, no significant additional effect was observed at the highest concentration; therefore, 100 pmol siRNA was determined to be the optimal concentration. Fig. 2A and B show a time-dependent response to the incubation with

100 pmol siRNAs following 24, 48 and 72 h of treatment with CLC-2-siRNA. The optimal time was determined to be 24 h. The results show that siRNA1 was the most effective siRNA at reducing the CLC-2 mRNA and protein expression levels.

*CLC-2 siRNA increases the expression levels of actin, vinculin and  $\beta$ -catenin.* Actin, vinculin and  $\beta$ -catenin were observed in normal HTM cell cultures and in transfected CLC-2-siRNA1 HTM cells by fluorescence microscopy, real time-PCR and western blot analysis. The predominant actin stress fibers were observed in almost all cells and were primarily aligned along the longitudinal axis of the cells (Fig. 3A). In the siRNA1 treated cells, the stress fibers were observed in certain cells; numerous cells contained a perinuclear, geodesic dome-like pattern of crosslinked actin filaments (Fig. 3F), which have previously been termed cross-linked actin networks (CLANs). Approximately half of the cells contained a variety of CLANs, ranging from a small perinuclear pattern to a network encompassing the entire cell (Fig. 3F). The actin fiber bundles were highly concentrated at the periphery of the cell, with a few actin filaments detected in the central area (Fig. 3F). Increased vinculin staining was also observed towards the cell periphery (Fig. 3G) compared with that in the untreated cells (Fig. 3B and C).

To investigate the effects of the CLC-2 siRNA1 on actin, vinculin and  $\beta$ -catenin mRNA and protein expression levels in the HTM cell line, HTM cells were treated with the CLC-2-siRNA1 for 24, 48 and 72 h. Actin, vinculin and  $\beta$ -catenin mRNA and protein levels were analyzed using real time-PCR and western blot analysis (Fig. 4). The relative quantification results show that the HTM cells transfected with the CLC-2 siRNA1 significantly induced the mRNA levels of actin, vinculin and  $\beta$ -catenin compared with that in the control group (Fig. 4A). Similar to the analysis of RNA levels, the protein levels of actin, vinculin and  $\beta$ -catenin were increased significantly in the siRNA1-treated cells compared with the control group (Fig. 4B).

*CLC-2 siRNA activates the TGF- $\beta$ /Smad signaling pathway in HTM cells.* Transforming growth factor- $\beta$  (TGF- $\beta$ ) is located in increasing quantities in the aqueous humor (AH) and reac-

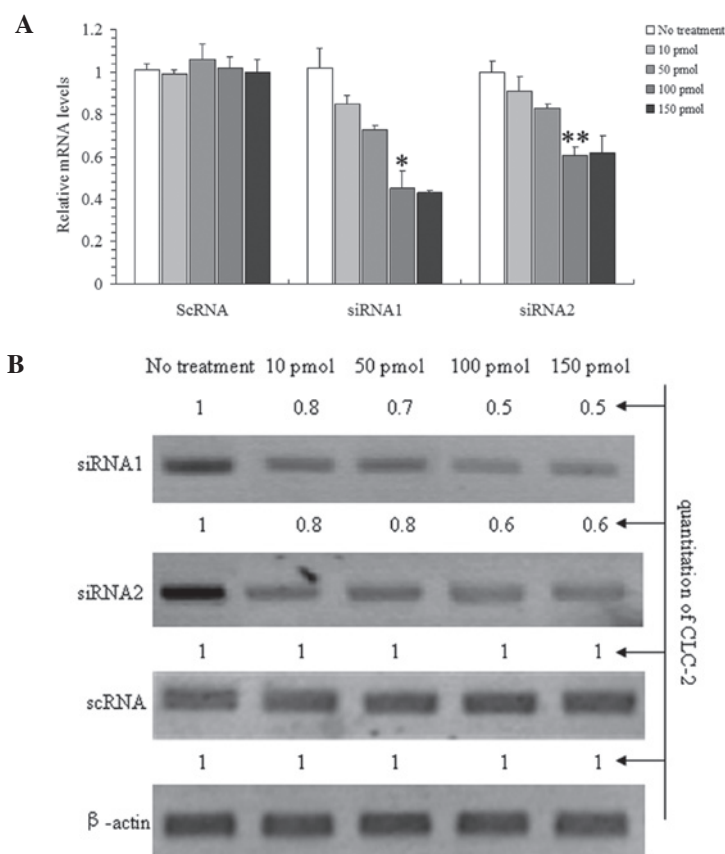


Figure 1. Effect of siRNA on the expression of CLC-2 in HTM cells. (A) The mRNA expression of CLC-2 was significantly inhibited by the different concentrations of siRNA. The cells were transfected with the indicated concentrations of siRNA1, siRNA2 or inactive scRNA for 24 h. The data are presented as the mean  $\pm$  SD of the normalized relative CLC-2 mRNA levels ( $n \geq 3$ ). \* $P < 0.05$ , compared with the control. (B) The CLC-2 protein expression was quantified via densitometry and compared with the no treatment control. The maximal grey value was set to 1 and all other results were expressed relative to this value (black) ( $n \geq 3$ ). CLC-2, chloride channel protein 2; HTM, human trabecular meshwork.

tive optic nerve astrocytes of patients with primary open-angle glaucoma (POAG) (17). The available data strongly indicate that TGF- $\beta$  is important in contributing to the structural changes characteristic of POAG in the extracellular matrix of the TM and optic nerve head (18). In addition, CLC-2 may function to stabilize the cytoskeleton. CLC-2 siRNAs were used to inhibit CLC-2 expression and the variation in TGF- $\beta$  levels was observed to investigate the correlation between CLC-2 and TGF- $\beta$  (Fig. 5). As shown in Fig. 5, compared with the control group, the expression levels of TGF- $\beta$  and Smad2 were increased when the expression of CLC-2 was reduced by CLC-2 siRNA. Compared with the 24 h exposure period, as the inhibition effects of CLC-2 siRNA declined, the expression levels of TGF- $\beta$  and Smad2 gradually reduced at 48 and 72 h; thus, these effects were dependent on CLC-2 expression levels. Based on these results, CLC-2 siRNA may contribute to TM cytoskeleton disorders and may be related to the TGF- $\beta$ /Smad signaling pathway.

## Discussion

In the eye, the predominant AH outflow pathway in humans is through the TM and Schlemm's canal, although ~20% of the AH leaves the anterior chamber in between the ciliary muscle fibers to reach the scleral tissue (18). These sections of the eye express high levels of cytoskeletal actin. The

cytoskeleton is comprised of a complex network of fibers that integrate various inclusions into the network to produce coordination among cells. The cytoskeleton is important in regulating cell morphology, extracellular matrix adhesion and cell movement (19). Cells adapt to changes in the surrounding environment by restructuring the actin cytoskeleton. Increasing actin cytoskeleton crosslinking reinforces the TM and increases the aqueous outflow; however, this increased outflow may lead to an obstruction and increase the intraocular pressure, thereby damaging the normal structure and function of the eye and resulting in the development of POAG (20).

Voltage-gated chloride channels of the plasma membrane are key in cell volume regulation, ionic homeostasis, transepithelial transport and the regulation of electrical excitability. Intracellular members of the chloride channel family are also involved in organellar volume regulation and electroneutrality maintenance. CLC-2 is a member of the large CLC family of chloride-channel forming proteins and may be important in TM cells (21-22).

In the present study, two siRNAs that target CLC-2 mRNA were designed as a potential novel genetic therapeutic strategy to inhibit the expression of CLC-2 and affect the cytoskeleton of HTM cells. The cytoskeleton was analyzed following an siRNA-mediated CLC-2 knockdown. The results demonstrated that siRNA1 and 2 were able to inhibit the expression of CLC-2. In direct comparison, siRNA1 was shown to be



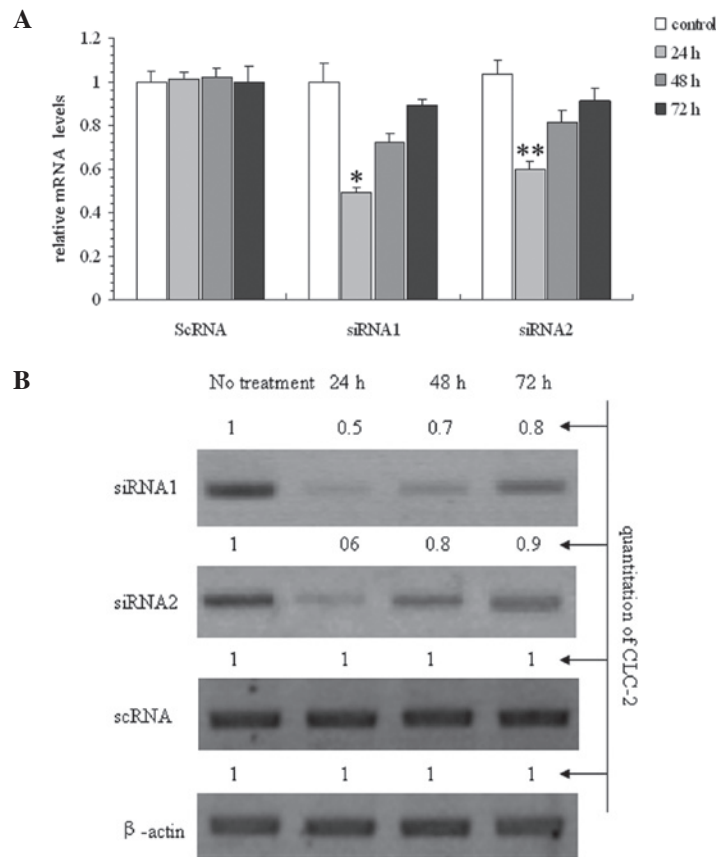


Figure 2. Effect of siRNA on the expression of CLC-2 in HTM cells. (A) The mRNA expression of CLC-2 was significantly inhibited by the siRNA. The cells received either no treatment or were transfected with 100 pmol of siRNA1, siRNA2 or scRNA for 24, 48 and 72 h. The data are presented as the mean  $\pm$  SD of the relative CLC-2 mRNA expression levels compared with the control (no treatment) ( $n \geq 3$ ). \* $P < 0.05$ , compared with the control. (B) The protein expression of CLC-2 was equally inhibited by siRNA1 and 2. The CLC-2 protein expression was quantified via densitometry and compared with the no treatment control group. The maximal grey value was set to 1, and all other results were expressed relative to this value (black). The 24 h transfection with the siRNA exhibited the strongest reduction in the CLC-2 protein expression levels ( $n \geq 3$ ). CLC-2, chloride channel protein 2; HTM, human trabecular meshwork.

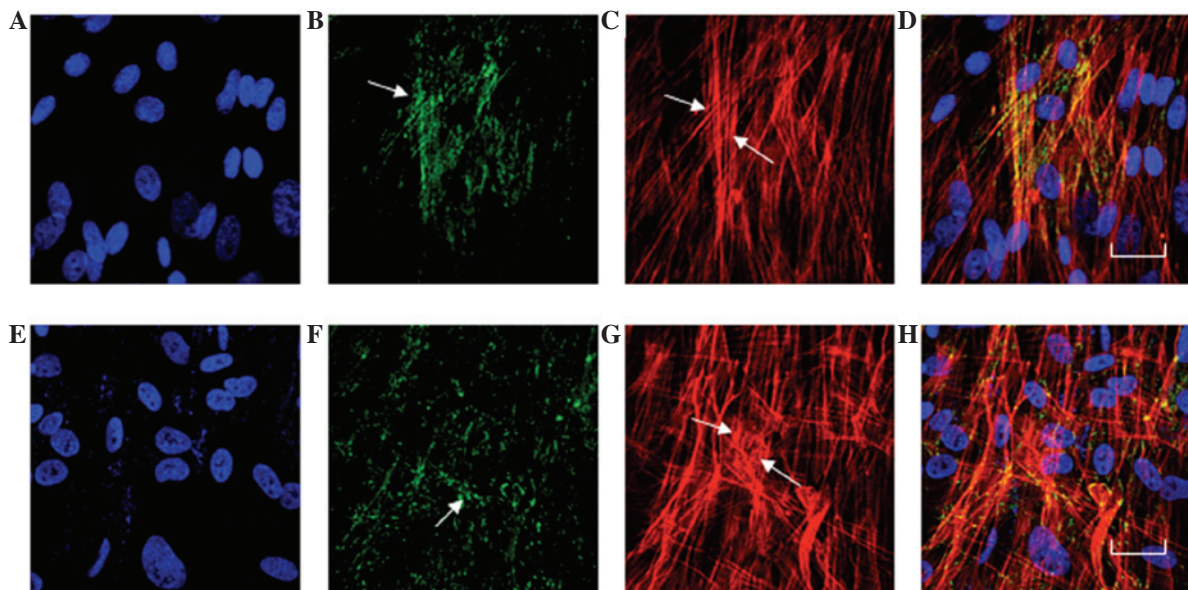


Figure 3. Effects of the CLC-2-siRNA on actin and vinculin in cultured HTM cells. The HTM cells were treated with (A-D) normal growth medium or (E-H) 100 pmol of the CLC-2-siRNA. (C) In the cells treated with normal growth medium, actin stress fibers were observed in almost all of the cells and were primarily aligned along the longitudinal axis of the cells. (F) In the cells treated with 100 pmol of the CLC-2-siRNA1 for 24 h, the vinculin was also observed. (G) In the cells treated with 100 pmol of the CLC-2-siRNA1 for 24 h, the actin fiber bundles were highly concentrated at the periphery of the cell, while a few actin filaments were detected in the central area. Increased vinculin staining was also observed toward the cell periphery. (H) CLC-2-siRNA treated HTM cells co-stained to visualize actin (red) and vinculin (green). The siRNA1 induced changes are shown by arrows. F and G, Bar=20  $\mu$ m. A-D, No treatment; E-H, CLC-2 siRNA treatment; A and E, DAPI staining; B and F, FITC staining; C and G, TRITC staining; D and H, Co-staining; CLC-2, chloride channel protein 2; HTM, human trabecular meshwork.

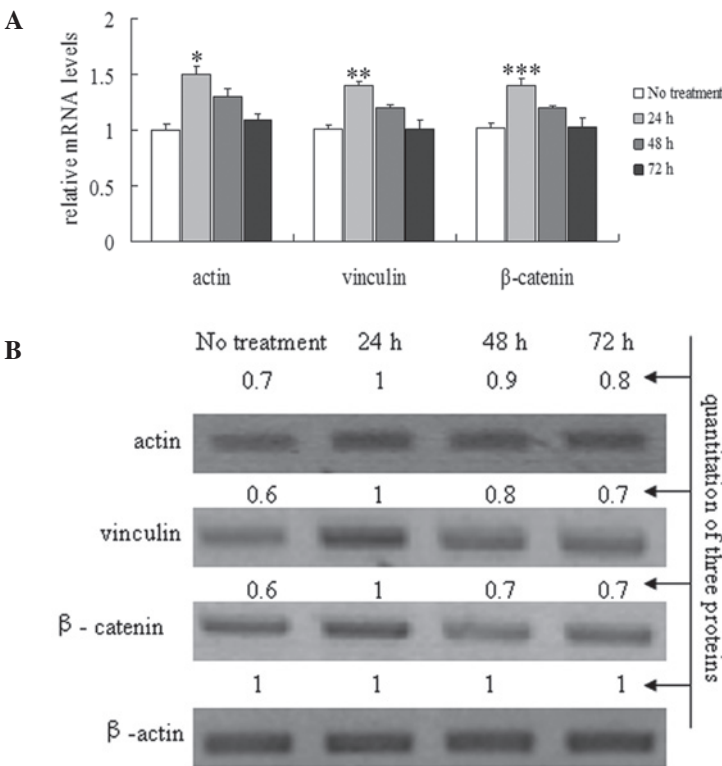


Figure 4. Effects of siRNA on the expression of actin, vinculin and β-catenin in HTM cells. (A) The cells were treated with 100 pmol of the siRNA1 for 24, 48 and 72 h. The total mRNA was subjected to qPCR to analyze the changes in actin, vinculin and β-catenin mRNA expression levels; β-actin served as a loading control. The data are presented as the mean ± SEM and were taken from three independent experiments (n=3). \*P<0.05, \*\*P<0.05 and \*\*\*P>0.05 vs. the control group. (B) HTM cells were transfected with the siRNA1 and the actin, vinculin and β-catenin expression levels were determined by western blot analysis for the 24, 48 and 72 h exposure periods. The results shown are representative of three repeated experiments. CLC-2, chloride channel protein 2; HTM, human trabecular meshwork.

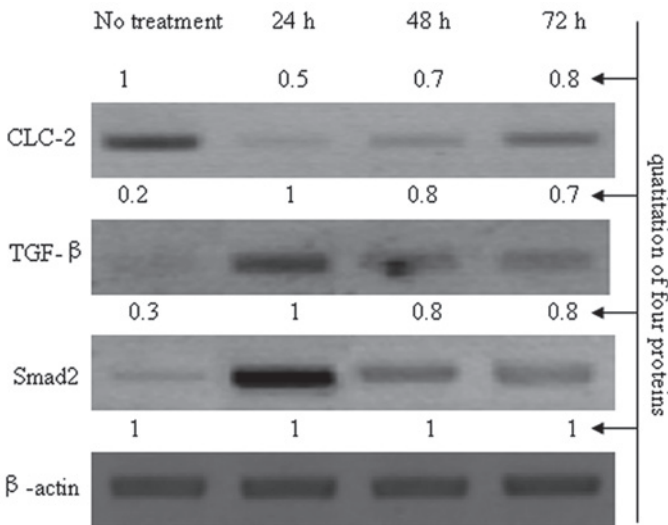


Figure 5. Effects of the siRNA on the expression levels of TGF-β and Smad2 in HTM cells. HTM cells were transfected with siRNA1 and the CCL-2, TGF-β and Smad2 expression levels were determined by western blot analysis at 24, 48 and 72 h. The results shown are representative of three repeated experiments. TGF-β, transforming growth factor-β; HTM, human trabecular meshwork; CLC-2, chloride channel protein 2.

more effective than siRNA2 in downregulating the expression of CLC-2. The results also showed that CLC-2 was related to the stability of the cytoskeleton, as the cytoskeleton became disordered when the expression levels of CLC were reduced in HTM cells. F-actin *in vitro* generally contains two types of fiber: stress fibers that are distributed in the parallel beam in

the cells and fibers that are distributed around the peripheral actin. Stress fibers arranged in the cell stretch the direction of the cell and peripheral actin maintains the form of cells and participates in the formation of the connection between the cell and the extracellular matrix. Fluorescence microscopy was used to observe the changes in actin organization in the

present study and the results showed that siRNA1-mediated CLC-2 knockdown reconstructed the actin cytoskeleton and formed CLAN structures. The reconstruction of the actin cytoskeleton changed the zonula occludens and gap junction protein expression levels and influenced the connection and adhesion of the cells. These changes affected the TM structure and function, and increased the TM aqueous outflow resistance.

TGF- $\beta$ 2 is the predominant TGF- $\beta$  in the eye and is located in large quantities in the aqueous humor of the anterior eye and in the vitreous, neural retina and retinal pigmented epithelium of the posterior eye. Only minor or non-detectable TGF- $\beta$ 2 expression levels have been observed in studies of the normal TM (17). In the aqueous humor of patients with POAG, the quantities of TGF- $\beta$ 2 have been observed to be significantly increased in several studies (19-20). The increase in the quantity of the expression of TGF- $\beta$ 2 appears to be a characteristic phenomenon in the eyes of patients with POAG (18). In the present study, the results demonstrated that siRNA1-mediated CLC-2 knockdown reconstructed the TM cytoskeleton and that CLC-2 knockdown-related cytoskeletal reconstruction may involve the TGF- $\beta$ /Smad signaling pathway. The initial analysis showed that the siRNA1-mediated CLC-2 knockdown significantly upregulated the expression levels of TGF- $\beta$  and Smad2. These results suggested that a CLC-2 knockdown may promote TM cytoskeletal disorders and may be correlated with the activation of the TGF- $\beta$ /Smad signaling pathway.

In conclusion, the results demonstrated the correlation between CLC-2 and the cytoskeleton in HTM cells. CLC-2 may be a promising potential novel therapeutic agent for combating POAG, and further studies are required to confirm these results.

## Acknowledgements

This study was partially supported by the National Natural Science Foundation of China (grant no. 81271002).

## References

- Thinda S, Melson MR and Kuchtey RW: Worsening angle closure glaucoma and choroidal detachments subsequent to closure of a carotid cavernous fistula. *BMC Ophthalmol* 12: 28, 2012.
- Abdelrahman AM and Eltanamly RM: Selective laser trabeculoplasty in Egyptian patients with primary open-angle glaucoma. *Middle East Afr J Ophthalmol* 19: 299-303, 2012.
- Roh M, Zhang Y, Murakami Y, *et al*: Etanercept, a widely used inhibitor of tumor necrosis factor- $\alpha$  (TNF- $\alpha$ ), prevents retinal ganglion cell loss in a rat model of glaucoma. *PLoS One* 7: e40065, 2012.
- Grieshaber MC, Pienaar A, Olivier J and Stegmann R: Clinical evaluation of the aqueous outflow system in primary open-angle glaucoma for canaloplasty. *Invest Ophthalmol Vis Sci* 51: 1498-1504, 2010.
- Kotliar KE, Kozlova TV and Lanzl IM: Postoperative aqueous outflow in the human eye after glaucoma filtration surgery: biofluidmechanical considerations. *Biomed Tech (Berl)* 54: 14-22, 2009.
- Wang N, Chintala SK, Fini ME and Schuman JS: Activation of a tissue-specific stress response in the aqueous outflow pathway of the eye defines the glaucoma disease phenotype. *Nat Med* 7: 304-309, 2001.
- Bomberger JM, Coutermarsh BA, Barnaby RL and Stanton BA: Arsenic promotes ubiquitinylation and lysosomal degradation of cystic fibrosis transmembrane conductance regulator (CFTR) chloride channels in human airway epithelial cells. *J Biol Chem* 287: 17130-17139, 2012.
- Zhu L, Yang H, Zuo W, *et al*: Differential expression and roles of volume-activated chloride channels in control of growth of normal and cancerous nasopharyngeal epithelial cells. *Biochem Pharmacol* 83: 324-334, 2012.
- Comes N, Abad E, Morales M, Borrás T, Gual A and Gasull X: Identification and functional characterization of CIC-2 chloride channels in trabecular meshwork cells. *Exp Eye Res* 83: 877-889, 2006.
- Földy C, Lee SH, Morgan RJ and Soltesz I: Regulation of fast-spiking basket cell synapses by the chloride channel CIC-2. *Nat Neurosci* 13: 1047-1049, 2010.
- Roman RM, Smith RL, Feranchak AP, Clayton GH, Doctor RB and Fitz JG: CIC-2 chloride channels contribute to HTC cell volume homeostasis. *Am J Physiol Gastrointest Liver Physiol* 280: G344-G353, 2001.
- Xiong H, Li C, Garami E, *et al*: CIC-2 activation modulates regulatory volume decrease. *J Membr Biol* 167: 215-221, 1999.
- Britton FC, Hatton WJ, Rossow CF, Duan D, Hume JR and Horowitz B: Molecular distribution of volume-regulated chloride channels (CIC-2 and CIC-3) in cardiac tissues. *Am J Physiol Heart Circ Physiol* 279: H2225-H2233, 2000.
- Thomasy SM, Wood JA, Kass PH, Murphy CJ and Russell P: Substratum stiffness and latrunculin B regulate matrix gene and protein expression in human trabecular meshwork cells. *Invest Ophthalmol Vis Sci* 53: 952-958, 2012.
- Zhou H, Tang Y, Liang X, Yang X, Yang J, *et al*: RNAi targeting urokinase-type plasminogen activator receptor inhibits metastasis and progression of oral squamous cell carcinoma in vivo. *Int J Cancer* 125: 453-462, 2009.
- Peng J, Lei CT, Hu JB and Fan YC: Effects of travoprost on actin cytoskeleton and  $\beta$ -catenin in the human trabecular meshwork cells treated with Dexamethasone. *Zhonghua Yan Ke Za Zhi* 47: 336-341, 2011 (In Chinese).
- Sethi A, Mao W, Wordinger RJ and Clark AF: Transforming growth factor-beta induces extracellular matrix protein cross-linking lysyl oxidase (LOX) genes in human trabecular meshwork cells. *Invest Ophthalmol Vis Sci* 52: 5240-5250, 2011.
- Fuchshofer R and Tamm ER: The role of TGF- $\beta$  in the pathogenesis of primary open-angle glaucoma. *Cell Tissue Res* 347: 279-290, 2012.
- Kottler UB, Jünemann AG, Aigner T, Zenkel M, Rummelt C and Schlötzer-Schrehardt U: Comparative effects of TGF-beta and TGF-beta 2 on extracellular matrix production, proliferation, migration, and collagen contraction of human Tenon's capsule fibroblasts in pseudoexfoliation and primary open-angle glaucoma. *Exp Eye Res* 80: 121-134, 2005.
- Cumurcu T, Bulut Y, Demir HD and Yenisehirli G: Aqueous humor erythropoietin levels in patients with primary open-angle glaucoma. *J Glaucoma* 16: 645-648, 2007.
- Grosheva I, Vittitow JL, Goichberg P, *et al*: Caldesmon effects on the actin cytoskeleton and cell adhesion in cultured HTM cells. *Exp Eye Res* 82: 945-958, 2006.
- Li A, Leung CT, Peterson-Yantorno K, Stamer WD, Mitchell CH and Civan MM: Mechanisms of ATP release by human trabecular meshwork cells, the enabling step in purinergic regulation of aqueous humor outflow. *J Cell Physiol* 227: 172-182, 2012.